Mobile surveys and machine learning can improve urban noise mapping: Beyond A-weighted measurements of exposure

Tatiana Alvares-Sanches[a,b], Patrick E. Osborne[c], Paul R. White[d]

[a]Faculty of Engineering and Physical Sciences, University of Southampton, Southampton SO17 1BJ, UK
[b]GeoData Institute, School of Geography and Environmental Science, University of Southampton, Southampton SO17 1BJ, UK
[c]School of Geography and Environmental Science, Faculty of Environmental and Life Sciences, University of Southampton, Southampton SO17 1BJ, UK
[d]Institute of Sound and Vibration Research, Faculty of Engineering and Physical Sciences, University of Southampton, Southampton SO17 1BJ, UK

Corresponding author:
Tatiana Alvares-Sanches
E-mail: t.a.sanches@soton.ac.uk
GeoData Institute, School of Geography and Environmental Science, University of Southampton, Southampton SO17 1BJ, UK

Abstract

Urban noise pollution is a major environmental issue, second only to fine particulate matter in its impacts on physical and mental health. To identify who is affected and where to prioritise actions, noise maps derived from traffic flows and propagation algorithms are widely used. These may not reflect true levels of exposure because they fail to consider noise from all sources and may leave gaps where roads or traffic data are absent.

We present an improved approach to overcome these limitations. Using walking surveys, we recorded 52,366 audio clips of 10 seconds each along 733 km of routes throughout the port city of Southampton. We extracted power levels in low (11 to 177 Hz), mid (177 Hz to 5.68 kHz), high (5.68 to 22.72 kHz) and A-weighted frequencies and then built machine-learning (ML) models to predict noise levels at 30 m resolution across the entire city, driven by urban form.

Model performance (r^2) ranged from 0.41 (low frequencies) to 0.61 (mid frequencies) with mean absolute errors of 4.05 to 4.75 dB. The main predictors of noise were related to modes of transport (road, air, rail and water) but for low frequencies, port activities were also important. When mapped to the city scale, A-weighted frequencies produced a similar spatial pattern to mid-frequencies, but did not capture the major sources of low frequency noise from the port or scattered hotspots of high frequencies. We question whether A-weighted noise mapping is adequate for health and wellbeing impact assessments.

We conclude that mobile surveys combined with ML offer an alternative way to map noise from all sources and at fine resolution across entire cities that may more accurately reflect true exposures. Our approach is suitable for noise data gathered by citizen scientists, or from a network of sensors, as well as from structured surveys.

Keywords: Noise pollution; noise modelling; spatial modelling; personal exposure; port city; urban environment

Introduction

Increasing urbanisation, population growth and the rise in vehicle use are leading to noisier urban environments, and historical documents leave little doubt that noise has long been an issue in cities (Goldsmith 2012). Despite this long history, environmental noise has not been studied or controlled to the same extent as other pollutants such as air pollution (Sørensen *et al.* 2012; EEA 2014; Murphy & King 2014a; King & Murphy 2016). According to the European Environment Agency (EEA) (2019), noise pollution is still a major environmental health issue in Europe, with road traffic being the major contributor, and the second most harmful environmental stressor after fine particulate pollution (WHO 2018; EEA 2019). Indeed, it is estimated that 100 million Europeans are affected by harmful levels of noise pollution (EEA 2019). Over recent years, there has been a considerable increase in the number of studies associating noise pollution with sleep disturbance (Douglas & Murphy 2016); annoyance (Laszlo *et al.* 2012; Guski *et al.* 2016; Fredianelli *et al.* 2019); decrease in cognitive performance among schoolchildren (Lercher *et al.* 2003; Chetoni *et al.* 2016); increased risk of preterm birth (Smith *et al.* 2020); psychological problems such as anxiety and depression (Beutel *et al.* 2016; van Kempen *et al.* 2018; Díaz *et al.* 2020); hearing loss and tinnitus (EEA 2014, 2019; Murphy & King 2014a); and hypertension and various cardiovascular diseases (Sørensen *et al.* 2012; van Kempen & Babisch 2012; Monrad *et al.* 2016; van Kempen *et al.* 2018; Andersson *et al.* 2020). As modern society develops, it has become urgent to understand the extent of environmental noise pollution, its impacts on humans and how to mitigate its effects. Indeed, if ways to control it are not sought, the impacts of noise pollution will increase at the rate of urbanisation (Murphy & King 2014a) with potentially serious consequences.

Within Europe, the 2002/49/EC Environmental Noise Directive (END) was formulated and implemented with the overall objective of identifying a common European Union (EU) approach to assessing exposure to environmental noise within Member States (Kephalopoulos *et al.* 2014; Murphy & King 2014a). Under the END, Member States are required to produce strategic noise maps for the assessment and management of noise exposure for all major roads, railways, airports and agglomerations. The outputs from these strategic noise maps are then used to determine the exposure of the population to noise under the terms of END (EC 2015) and to identify areas that need to be prioritised in action plans for noise reduction (Abramic *et al.* 2017; Kumar *et al.* 2020). The implementation of END has undoubtedly been an important stepping-stone in addressing and managing noise pollution at a continent-wide scale.

Despite this, there are limitations in the way noise maps are created that require further work. The methods used to calculate noise levels to produce strategic noise maps are primarily driven by annual traffic flows data from roads, railways and aircraft. Yet there is no established method to do this and different countries use different algorithms, input assumptions and parameters to produce their noise propagation calculations (European Environment Agency 2019; Murphy *et al.* 2020; Picaut *et al.* 2020). More fundamentally, environmental noise as defined under the END only takes into account noise emitted by certain means of transport. However, noise pollution in urban environments stems from a combination of noises from a multitude of sources (e.g. work places such as construction sites and ports, various types of machinery, sirens and horns from vehicles, and recreational venues such as music concerts). Noise maps could be improved if they considered the impact of combined sources of noise and the inclusion of annoyance indicators using spectral and temporal attributes of noise (Morel *et al.* 2016).

One particular omission is the failure to include shipping and port activities despite research showing that residents living in surrounding areas are negatively affected (Schenone *et al.* 2016). Indeed, more research has been done on the noise produced by vessels under the water than the air-borne noise they create in ports (Licitra *et al.* 2019). In addition to the noise emitted by ships during port approaches and while manoeuvring, once docked they continue to be a source of noise pollution due to the auxiliary engines and ventilation systems that are kept running (Badino *et al.* 2016). Activities associated with loading cargo and traffic around the port are also responsible for further levels of noise generated from port related activities (Schenone *et al.* 2016). Particularly during the night, noise levels may be above the night-time threshold guidelines recommended by the WHO and can be one of the main causes of sleep disturbance among local residents (Murphy & King 2014b).

While most attempts to map noise use modelled surfaces from sound propagation algorithms (Cai *et al.* 2015; Gulliver *et al.* 2015; DEFRA 2016; Wang *et al.* 2016; Bouzir & Zemmouri 2017), others have used actual recorded data, generally from static recording stations deployed across the city (Murphy & King 2014a; Hong & Jeon 2017; Sakieh *et al.* 2017; Han *et al.* 2018). Attempts have also been made to collect sound data on the move, focused on specific areas or neighbourhoods (Can *et al.* 2014; Murphy & King 2016) or more recently entire cities (Alvares-Sanches *et al.* 2019). Developing mobile survey methods could be important because it opens the way to collect sound data over large areas using citizen-scientists armed with smartphones, even in countries where official noise data are lacking. Although smartphone Apps and microphones are not yet sufficiently accurate for noise mapping, their further development offers promise for the near future (Kardous & Shaw 2016; Murphy & King 2016), including noise perception studies (Ricciardi *et al.* 2015). One issue with citizen-

science sound recordings is lack of control over the locations sampled and methods are needed to use such data efficiently for noise mapping. Although interpolation is often used to generalize sampled point measurements of sound data to yield mapped products (Can *et al.* 2014; Khan *et al.* 2018; Alvares-Sanches *et al.* 2019), such methods have inherent limitations. Foremost among these is spatial smoothing between points with no regard to the intervening land use and land cover. Although this can be partially overcome with approaches such as co-kriging, we present in this paper a non-parametric, machine-learning solution analogous to so-called land use regression as used in air quality and some noise modelling (Dons *et al.* 2013, 2014; Khan *et al.* 2018). In addition, we apply this method not only to map noise levels within the audible range of frequencies, but also to present noise maps for frequencies above and below this range. The consideration of frequencies outside the audible range is important due to the growing body of evidence on the impacts they may have on health (Castelo Branco 2001; Leighton 2016; Zhang *et al.* 2016; Fletcher *et al.* 2018; Scholkmann 2019). To consider the neglected issue of port cities, we conducted our study in Southampton which has some of the busiest container ports and passenger terminals in the UK. We suggest that the methods presented here augment current noise mapping such as defined in the END, providing more detail over extended areas on the levels of noise actually experienced by city users and across the sound spectrum.

Methods

Study area

The survey was carried out in the city of Southampton, UK and covered the whole area (51.8 km^2) within the administrative boundaries of the City Council. The city is located on the south coast of England at the top of the Solent. The waters of this strait feature prolonged high tides that create the ideal conditions for the transit of large ships, enabling Southampton to be a major port city in terms of both container and cruise passages. In recent years, Southampton has seen considerable transformations in its urban form, mostly within the city centre, and it is likely that future increases in the density of its built environment will result in a more compact and busier city. Although a large part of Southampton is dominated by impervious land surfaces, well-distributed green spaces account for just over 20% of the city's area.

Survey design

Sound surveys were conducted by walking surveyors on weekdays during the period 14 July to 25 August 2016, within three different time periods: morning rush hour (7:00 - 9:00), afternoon (13:00 – 15:00) and evening rush hour (16:30 – 18:30). During each time period, surveyors made continuous recordings of the acoustic environment along walked routes. Surveys were not carried out on windy or rainy days, although variations in local wind during surveys were inevitable. To minimise impacts on recordings, surveyors wore soft sole shoes, soft clothes, avoided accessories such as necklaces, and walked at a constant pace. Surveys were loosely structured spatially (i.e. into large regions of the city) using a land cover classification that divided the city into 10 potentially different sound zones based on the characteristics of the urban form. The idea was to prioritise routes that would include a mix of sound zones while also covering the city geographically. This semi-structured form of sampling was preferable to the use of fixed routes which, in any case, would soon break down due to the difficulties of sampling in some areas.

Recordings of the acoustic environment were made using Fostex FR–2LE and TASCAM DR–40 recorders, with PCB sensor signal conditioners (model 480E09) and PCB microphones (models: 377B02 & 377B11) with windshields. Surveyors carried the equipment inside rucksacks, with the microphone mounted above shoulder height at 1.65 – 1.70m. Microphones were calibrated using a Brüel & Kær sound level calibrator type 4230 emitting 94 dB at 1000 Hz to allow estimation of true decibel levels ("end-to-end calibration" in Merchant *et al.* 2015). The sampling rate was set to 96 kHz to allow coverage of sounds up to 48 kHz in theory, but limited in practice to 22.7 kHz due to microphone sensitivity. The location of each of the walking observers was logged every ten seconds as a track using Garmin Oregon 400t GPS receivers.

Sound data processing

Survey tracks were imported into ArcGIS 10.3 (Redlands, CA), where they were cleaned, converted into feature points and projected to the British National Grid (BNG). Audio files were imported into version 2.1.2 of Audacity (www.audacityteam.org) for visual and audio analysis. Sections of the audio files that showed unexpected clipping (e.g. from wind gusts) were removed and the precise timings of the removed sections noted. The audio files were then processed using custom-written code in MATLAB – R2016a to calculate the power levels in octave bands according to the ISO standard, for every 10 second period of each recording. The processed audio files were joined to the GPS location data using the time stamp on each to the nearest second. The power levels for each octave band and coordinates for each location were then exported to ArcGIS for plotting and modelling. Four different

response variables were derived from the sound data for this study because these had previous been shown to have distinctive characteristics (Alvares-Sanches *et al.* 2019). There were: low frequencies (11 to 177 Hz); mid frequencies (177 Hz to 5.68 kHz); high frequencies (5.68 to 22.72 kHz); and overall A-weighted power level (dBA).

Predictor variables

A set of 55 predictor variables that capture aspects of urban form were used in the predictive machine learning models (summarized in Table 1 and detailed in Appendix A). In addition, predictors for road transport were needed because traffic is widely acknowledged to be the dominant source of noise within the urban environment (Sørensen *et al.* 2012; EEA 2014; Weber *et al.* 2014; Brown 2015; Abramic *et al.* 2017; Alvares-Sanches *et al.* 2019). At the time of the analysis, the only traffic data available came from just 70 locations across the city and therefore these were first used to build a traffic submodel, capable of predicting traffic flows for the entire road network in Southampton (Appendix B). The outputs from this submodel were used as predictors in the sound models.

Table 1. Summary of the 55 predictor variables used, all generated at 30 m resolution. See Appendices A & B for details.

Variable type	Description
Land surface composition	Proportion of area composed of buildings, natural surfaces, hard surfaces, water bodies and unclassified mixed surfaces. Calculated for each 30 m pixel and in annuli 30-60 m, 60-90 m and 90-12 0 m around each pixel
	Normalized difference vegetation index (NDVI) derived from airborne RGBi imagery
	Proportion of area covered in low vegetation (<1 m), shrubs (1 m – 3 m) or trees (>3 m)
Vertical structure	Mean building height
	Sky view factor with search distances of 10 m and 100 m
	Positive and negative openness with search distances of 10 m and 100m
Terrain	Elevation, slope and aspect
Distance metrics	Euclidean distance from the centre of the pixel to the (nearest) airport, city centre, major road, minor road, motorway, motorway junction, port entrance, port or docks, rail track, water body, and flightpath (as projected on the ground)
Traffic	Modelled mean and maximum of traffic counts on roads within the pixel (see Appendix B for derivation)

Wind speed and direction were included in the sound models as confounding variables – i.e. they may affect the model outcome but are not predictors in the same sense as sources of sounds. Wind data were needed to match precisely the day and time of each sound clip and were sourced from Weather Underground (Wunderground.com) from five weather stations scattered across the city with reliable records. The procedure used to derive the wind variables in given in Appendix C.

The time of the survey was also treated here as a confounding variable because the same urban form may experience different sound levels at different times of time. As most pixels were surveyed on multiple occasions, the mode of the periods when surveys were conducted in each pixel was used in the models as an indicator of the main time of day influencing the outcome. In practice, time of day was not an important predictor (see later).

Model building

Predictive models for the means of low, mid and high frequencies, and dBA within each 30 m pixel were built using boosted regression trees (BRTs) within the R package gbm version 2.1.4 (Greenwell *et al.* 2018) together with the custom-written package BRT available as supplementary material to Elith *et al.*(2008b). BRTs are a relatively new statistical approach that stem from both machine learning (ML) and traditional statistical techniques (Elith *et al.* 2008a). In addition to their strong predictive performance, BRTs are advantageous because they can handle data of any type (categorical, numeric, binary, among others) and non-linear relationships among variables. They are insensitive to outliers and can accommodate variables containing missing attributes via classification (Elith *et al.* 2008a; Grus 2015; James *et al.* 2017). Model outcomes are not affected by transformations performed on the data and by the different measurement scales that predictors can take (Elith *et al.* 2008a). In addition, BRTs use boosting, a powerful method designed to fit sequentially several small models to the training data which together minimise the loss function and thus improve model accuracy (Elith *et al.* 2008a; Hastie *et al.* 2009; Elith & Leathwick 2017).

BRTs require three parameters to be tuned. Tree complexity (tc) controls the depth of interaction between the variables, learning rate (lr) determines the contribution of each tree to the growing model, and nt is the number of trees used (Elith *et al.* 2008a). In this paper, a grid search approach was used to find tc and lr over the ranges 4, 5, and 6 for tc and 0.1, 0.01 and 0.001 for lr. The combination of tc and lr was chosen to minimise the cross-validated deviance while keeping nt above 1000 (Elith *et al.* 2008a). Ten-fold cross-validation was used to tune model parameters and to select which variables to use (model simplification) from within a training sample of 80% of the data. In this way, 20% of the data was always held out from both model tuning and training, and it therefore

formed an effective independent testing sample. Model fit was assessed using r^2 and the mean absolute error (MAE).

To assess relative variable importance in the models, the most important variable was given a value of 100% and all others were evaluated relative to that score (Elith *et al.* 2008a; Hastie *et al.* 2009). Once the important predictors were known, the shape of their relationship with the response variable was visualized using partial dependence plots (Friedman 2001) which represent the effect of a predictor on the response when all other predictors are held at their average values. Partial dependence plots were plotted for the six most important variables, excluding the confounding variables.

The entire model building process is shown in Figure 1.

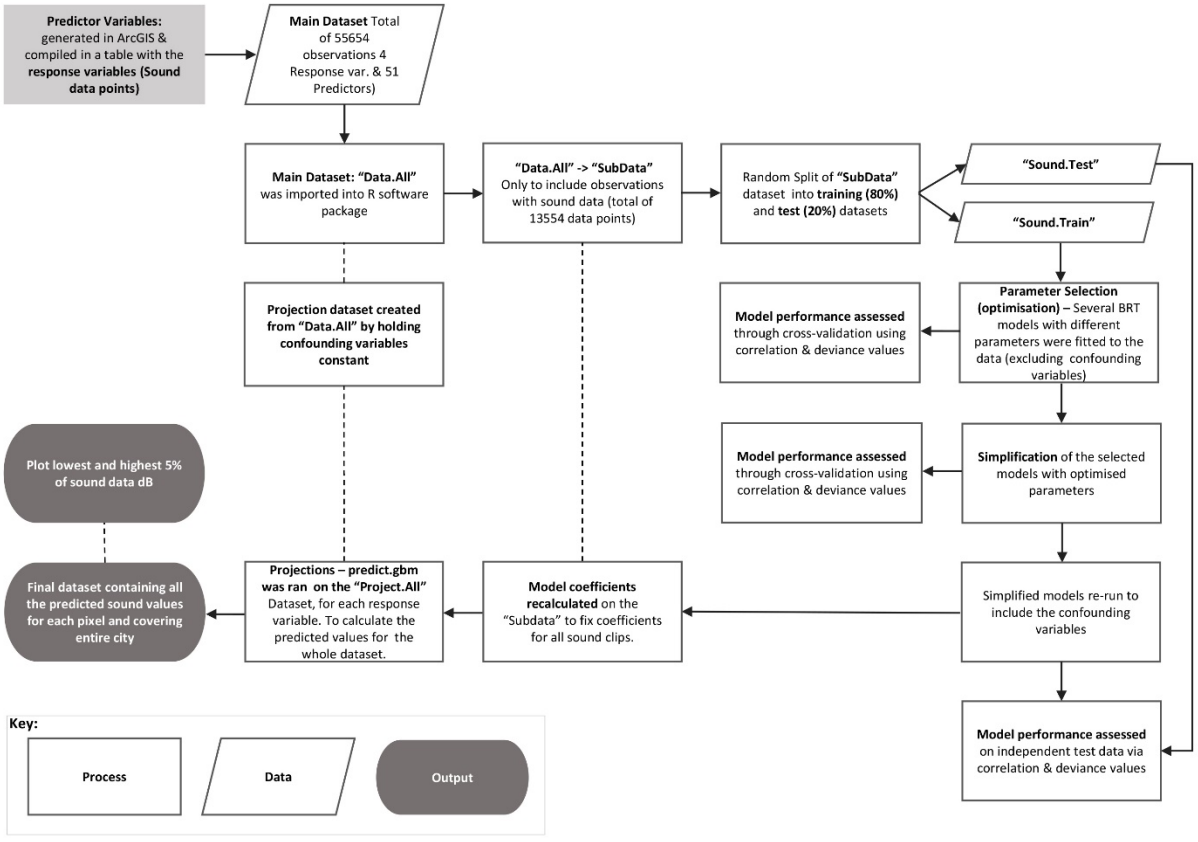

Figure 1. Workflow of the model building and fitting process for all of the response variables.

Results

Overall, the survey resulted in 52,366 georeferenced data points from 733 km of walked routes (based on an average speed of 1.4 m/s) with associated sound pressure levels, the powers of which were linearly averaged to form 13,554 pixels at 30 m resolution. These represent 24% of all pixels within the administrative boundary of the City of Southampton.

Results of the grid search for the best combination of parameter values for tree complexity (tc) and learning rate (lr) for each response variable consistently gave tc = 6 and lr = 0.01 but the number of fitted trees varied between 7,100 and 10,200 (Table 2). Models achieved typically optimistic r^2 values on the training data (0.66 to 0.89) that reduced to 0.31 to 0.55 when cross-validated (Table 2; row 4). The weakest model was for low frequencies and the equal best for mid frequencies and dBA. Backwards elimination of low contributing variables reduced the number of retained predictors to between 11 and 17, and the recalculated cross-validated r^2 values increased slightly for all bands (Table 2; row 7) but especially for the low frequencies. The addition of the confounding variables (wind and time period) led to modest increases in r^2 when applied to the independent test data set (Table 2; row 8). The final models showed mean absolute errors (MAE) of 4.05 to 4.75 dB for low to high frequencies and 4.18 dBA for the A-weighted frequencies.

Table 2. Summary of the selected models for each sound response variable and measures of their performance. MAE = mean absolute error.

	Low	**Mid**	**High**	**dBA**
Learning rate	0.01	0.01	0.01	0.01
Tree complexity	6	6	6	6
No. of trees before simplification	10150	9950	7100	10200
Cross-validated r^2 before simplification	0.31	0.55	0.41	0.55
No. of predictors after simplification	14	12	17	11
No. of trees after simplification	12100	11850	10950	12550
Cross-validated r^2 after simplification	0.37	0.58	0.44	0.58
Test r^2 after simplification and including confounding variables	0.41	0.61	0.46	0.61
Test MAE after model simplification and including confounding variables	4.05	4.23	4.75	4.18

Selected predictor variables

The most influential predictors across all response variables were predominantly related to means of transport i.e. road, air, rail and water (Table 3). The dominance of variables related to road traffic (traffic counts, distance to motorways and major roads, and hard surfaces), indicates its importance as the main source of noise in the city. Although the distance to the airport and flightpath featured in all models, they were more relevant to the low frequency bands, especially distance to flight path (Table 3). The presence of the distance to the port/ferry and water predictors could imply that port-related activities are also an important contributor to urban noise in Southampton (Table 3).

Wind speed and direction were the most important confounding variables, particularly in the low frequency bands (Table 3). While higher wind speeds may genuinely contribute to urban noise (e.g. by knocking objects together, rustling leaves on trees), a main effect could be inadequate shielding of the microphone, a view supported by the dominance in the low frequency bands. To compensate for this, wind speed and direction were held constant at their average values when the models were projected across the entire city (below). Likewise, although the influence of survey period was modest (Table 3), all pixels were classified with the commonest time of the day (morning) when models were projected.

Figures 2 to 5 show the partial dependence plots (PDP) for the six most important predictor variables for each response variable. The curves must be interpreted cautiously where the data are sparse (indicated by the rug plot of deciles on the top of each plot) and in all cases as the interaction depth (tree complexity) in the models was high. The spatial version of the traffic count model (Traffic_SpatialMax) played an important role in explaining urban noise at lower frequencies, there being a clear increase in noise with the increase of traffic counts up to just below 20,000 vehicles. Low frequency sounds also tended to increase with distance from the airport. This might suggest that noise in the low frequencies tends to be more affected by activity in the city centre and the port (away from the airport) rather than at the airport itself. In relation to sky view factor (SVF), an obstructed sky was related to a decrease in noise intensity in the low frequency bands, with an inverted effect in SVF values from 0.5 onwards.

280 Table 3. Predictor variables retained in the simplified models for each response. The top half of the
281 table shows the rank importance order of the predictors, excluding the confounding variables. The
282 bottom half of the table gives the original rank order of the confounding variables when together with
283 the predictors. Variable names are decoded in Appendices A and B.

Predictor Variables	**Description** (derived in Appendices A and B)	**Low**	**Mid**	**High**	**dBA**
Traffic_SpatialMax	Output from the spatial traffic counts (MARS model, Appendix B) using "maximum value rule" when assigning a count to each 30 m pixel	1	3	4	3
Dist_Airport	Euclidean distance of each pixel to the airport	2	4	3	4
SVFR10D32	Sky view factor, search distance of 10 m in 32 directions	3			
Hrd_Ann12	Proportion of hard surfaces in 30-60 m annulus	4	2	2	2
Dist_Motorway	Euclidean distance to the motorway	5	8	6	7
Dist_FlightPath	Euclidean distance to the flight path	6	10	17	8
Dist_PortDocks	Euclidean distance to the port or docks	7	9	15	11
Nat_Ann34	Proportion of natural surfaces in 90-120 m annulus	8	11	12	10
Dist_Rail	Euclidean distance to rail tracks	9	5	5	5
Hard_Ann23	Proportion of hard surfaces in 60-90 m annulus	10			
Dist_WaterAll	Euclidean distance to all water bodies	11			
Dist_WaterME	Euclidean distance to all water bodies with the presence of motorised engines	12	12	16	
Dist_MajorRds	Euclidean distance to major roads	13	1	1	1
Mix_Ann23	Proportion of mixed surfaces in 60-90 m annulus	14			
Traffic_AspatialMax	Output from the aspatial traffic counts (MARS model, Appendix B) using "maximum value rule" when assigning a value to each 30 m pixel		6	7	6
Dist_Water	Euclidean distance to water bodies (excluding those with motorised engines)		7	11	9
VLC_Ground	Vegetation land cover at ground level			8	
Traffic_AspatialMean	Output from the aspatial traffic counts (MARS model, Appendix B) using "mean value rule" when assigning a value to each 30 m pixel			9	
Bldg_Ann12	Proportion of buildings in 30-60 m annulus			10	
Mix_Ann12	Proportion of mixed surfaces in 30-60 m annulus			13	
Hrd	Proportion of hard surfaces in each 30 m pixel			14	
Confounding Variables					
WindSpeed	Average wind speed	1	6	6	8
WindDir_Cos	Average wind direction (cosine)	5	11	7	12
WindDir_Sin	Average wind direction (sine)	6	5	3	7
ModalPeriodDay	Modal survey period	18	16	18	15

284

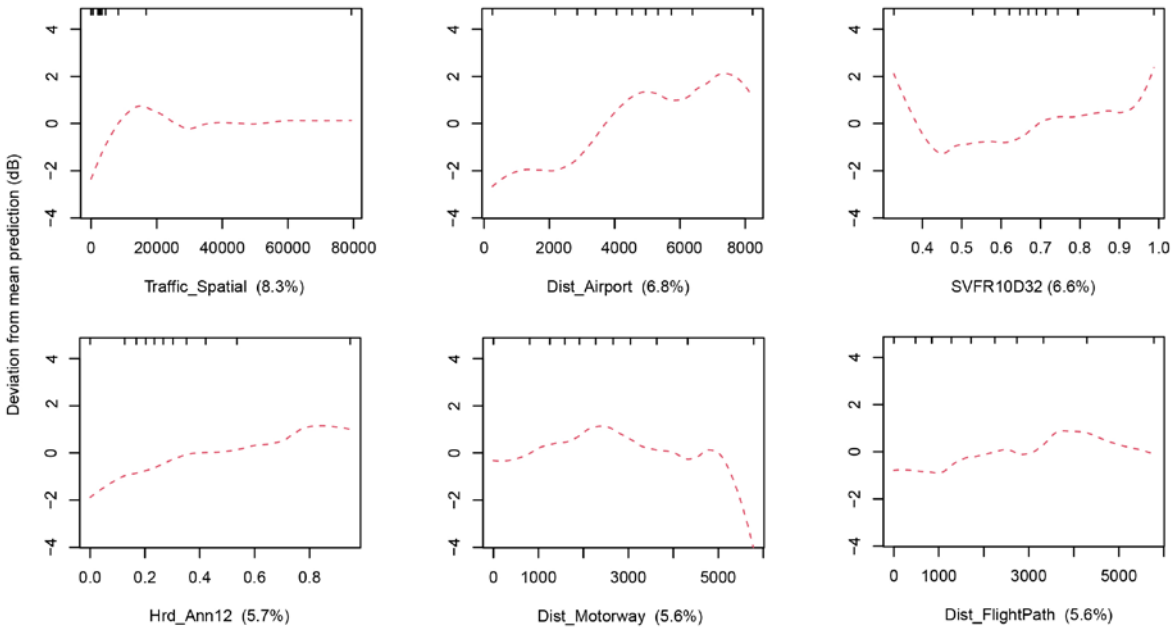

Figure 2. Partial dependence plots of the six most relevant predictor variables in the model for the low frequencies. Rug plots are shown at the top of each plot and represent the distribution of sample points across that variable, in deciles.

The PDPs for mid frequencies and dBA were very similar (Figures 3 and 4), indicating strong influences from road traffic, major roads, hard surfaces (which are generally motorable), rail transport and proximity of the airport (but with a complex pattern as for low frequencies).

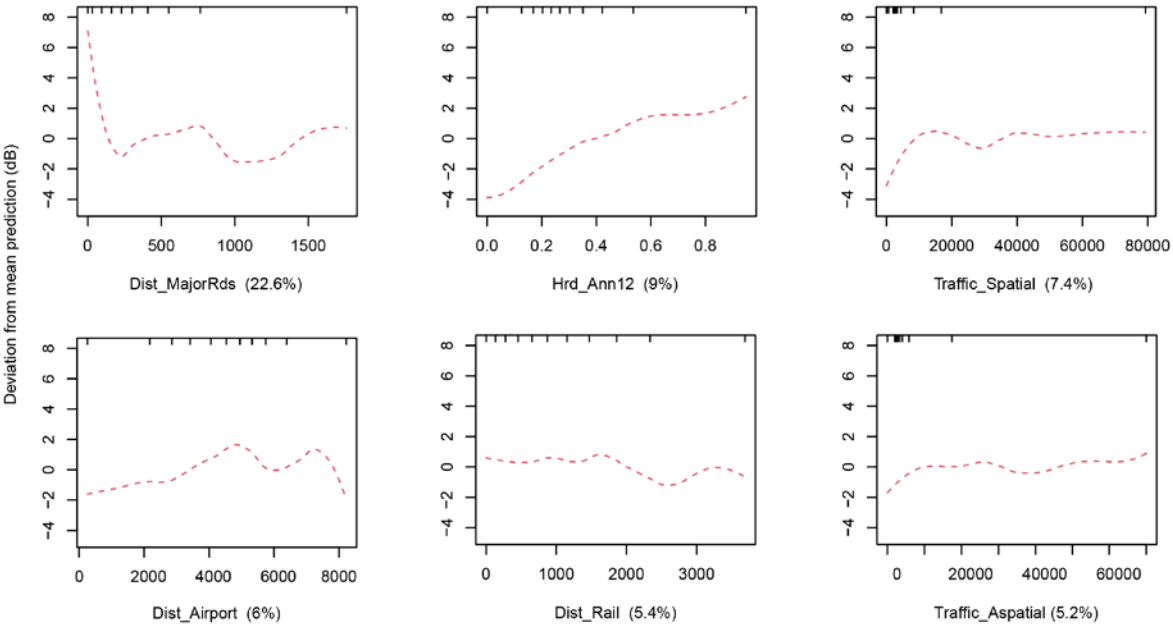

Figure 3. Partial dependence plots of the six most relevant predictor variables in the model for the mid frequencies. Rug plots are shown at the top of each plot and represent the distribution of sample points across that variable, in deciles.

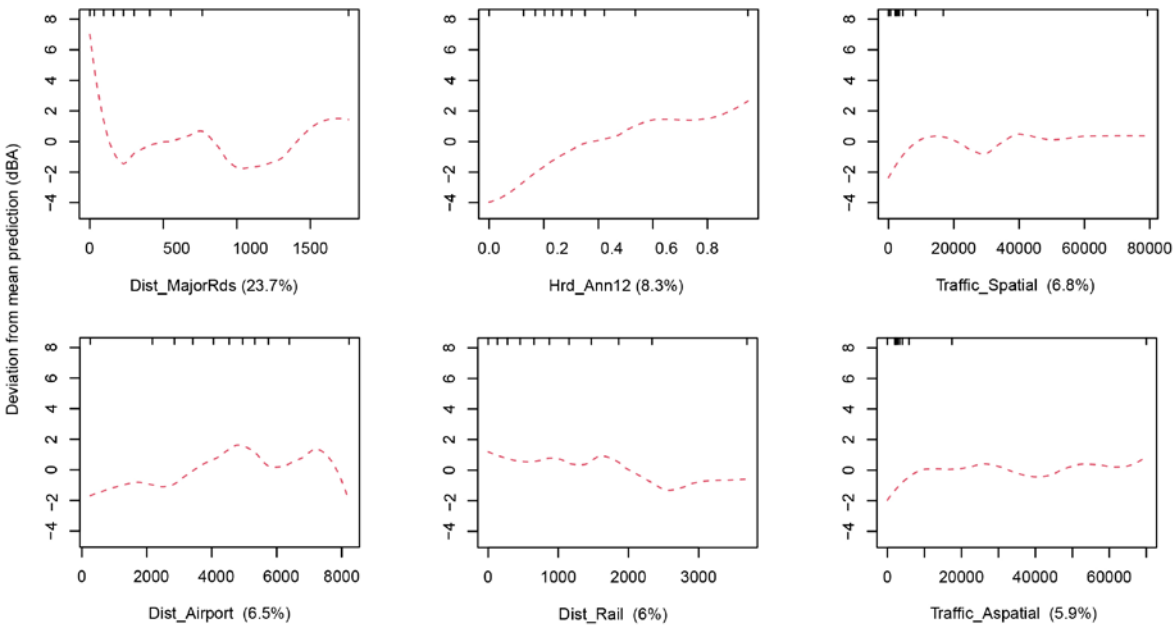

296

297 Figure 4. Partial dependence plots of the six most relevant predictor variables in the model for dBA.
298 Rug plots are shown at the top of each plot and represent the distribution of sample points across that
299 variable, in deciles.

300 High frequencies also tended to occur immediately next to major roads but sharply declined by 250 m
301 away, and also within areas with a high percentage cover of hard surfaces (Figure 5). As with the other
302 frequency bands, high frequencies were affected by the presence of road traffic. Rail tracks and trains
303 may also be a source of high frequency noise in urban areas as the influence declined with distance
304 (Figure 5).

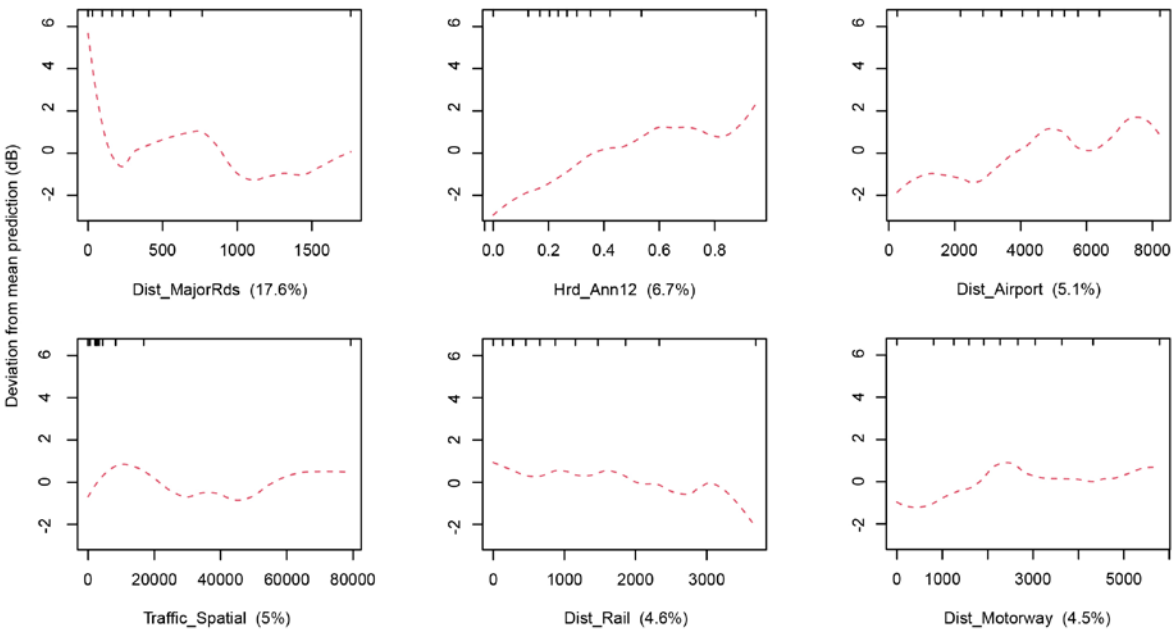

Figure 5. Partial dependence plots of the six most relevant predictor variables in the model for the high frequencies. Rug plots are shown at the top of each plot and represent the distribution of sample points across that variable, in deciles.

Projected noise maps

When projected across the entire city, the low frequencies noise map (Figure 6, top left) showed sound pressure level (SPL) values ranging between 56 and 85 dB. These are mean dB levels throughout the day. The area of the docks was consistently noisy in the low frequency bands, suggesting that port activities such as the manoeuvring of cranes, presence of trucks and large containers ships, are sources of low frequency noise. The road network is also visible but is rather indistinct, with little differentiation between major and minor roads, in contrast to other frequency bands. The projected noise maps for mid frequencies and dBA (Figure 6, top and middle right) showed very few differences between them. They clearly have a spatial pattern where the road network stands out distinctly, especially the major roads which appear to be among the noisier areas of the city. This is consistent with the information provided the by PDPs (Figures 3 and 4) that link noise intensity with the presence of motorised vehicles. Sound pressure levels ranged between 38 dB and 71 dB for mid frequencies, and 42 dBA to 77 dBA for the dBA map. The spatial similarity between the dBA and mid frequency maps is mirrored in the frequency distributions of their sound pressure levels (Figure 7), whereas low and high frequencies are characterised by higher and lower SPLs respectively. Although the city was generally quieter in the high frequency bands (SPL range: 20 to 50 dB), the road network still stands out, alongside the port (Figure 6, middle left). The area around the city centre is also pronounced in the high frequency bands but less so at lower frequencies, suggesting sources other than road traffic

(for example, shops or high pedestrian footfall) may be responsible. When compared with the published strategic noise maps (Figure 6, bottom row) which are recoloured here to use the same palette as for dBA, the values observed for the major roads fall within a similar range, but projections are lacking for much of the city.

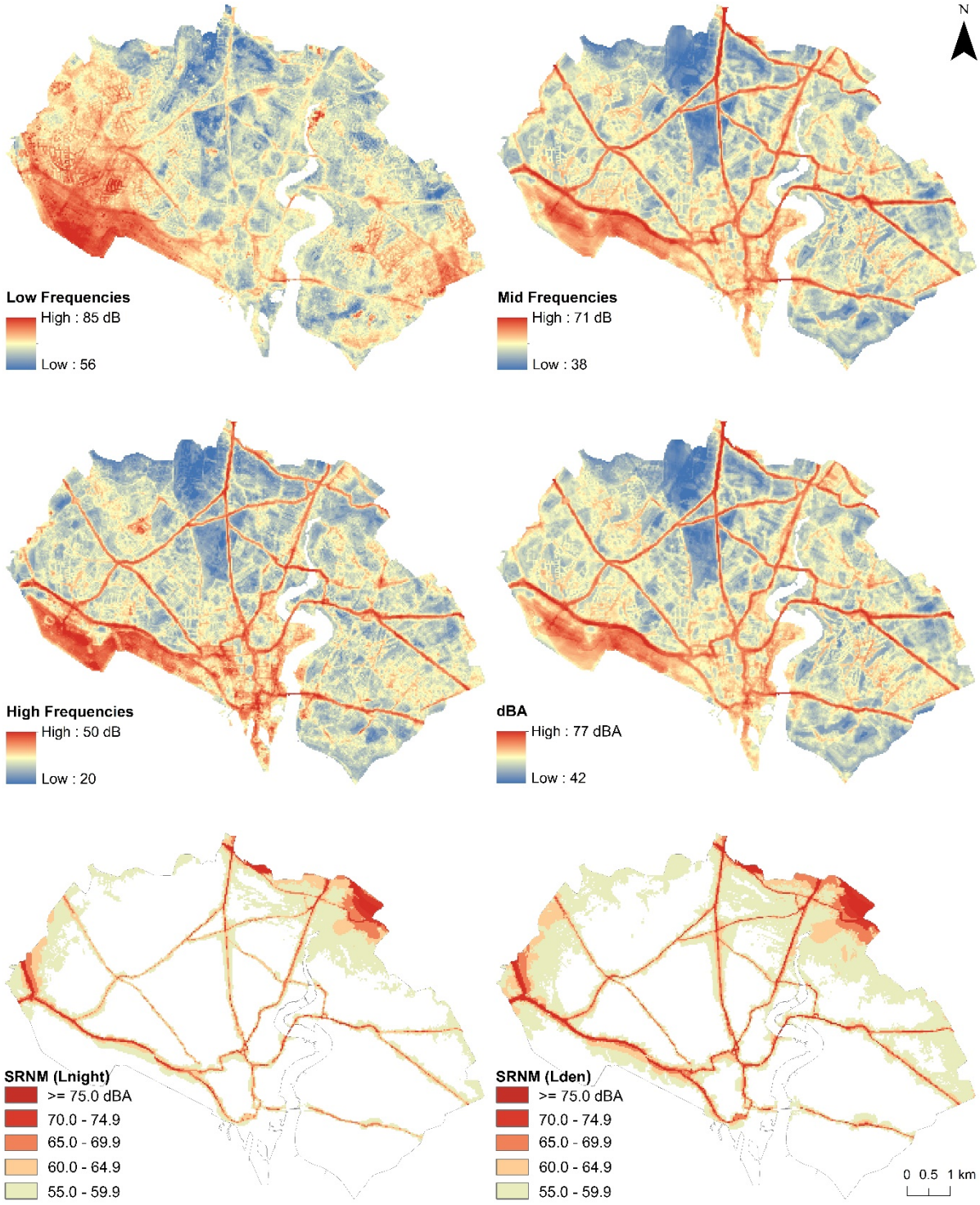

Figure 6. Projected noise maps for low (top left), mid (top right), high frequencies (middle left) and dBA (middle right), compared with the published strategic road noise maps (bottom row) from DEFRA

(2020a, b). SRNM (Lnight) is the annual average noise level between 23.00 – 07.00, and SRNM (Lden) is the annual average noise level with separate weightings for the evening and night periods.

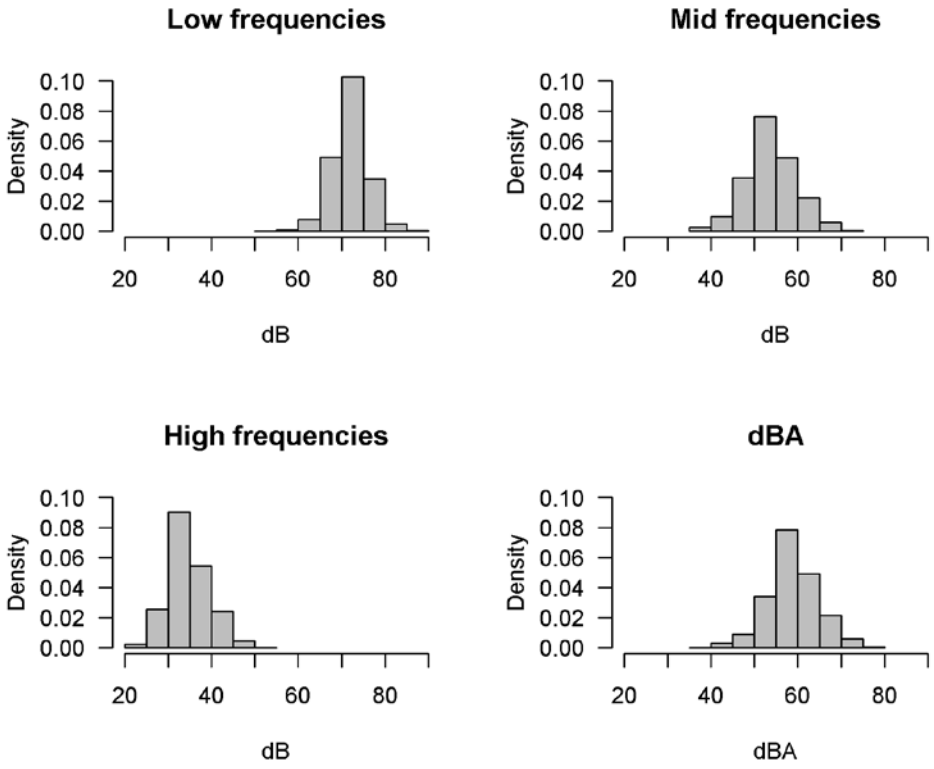

Figure 7. Frequency distributions for projected noise levels in low (top left), mid (top right) and high frequency (bottom left) bands, plus dBA (bottom right).

Identification of the noisiest and quietest areas by frequencies

The SPLs of the quietest 5% of pixels varied between 56 – 66 dB for the low frequencies, 38 – 44 dB for the mid frequencies, and between 20 – 27 dB for the high frequencies (Figure 8). The overall patterns of the quietest 5% of pixels were broadly similar across the frequencies and often match the areas of greenspace or their immediate surroundings in the city. However, it is noticeable that the quietest 5% for the mid frequencies occur in more solid blocks and are less dispersed than those for low or high frequencies. Some of the quieter areas at low frequencies may be related to tree cover. For example, on an area known as the Common, most of the area covered by a relatively dense canopy of trees is quieter than the areas of open grass without trees. Figure 7 (bottom right), also maps all areas of the city quieter than 55 dBA (in light green) as specified by the END for noise mapping and action planning (DEFRA 2015). This is more extensive than the quietest 5% for dBA and increases substantially the number of areas defined as having an acceptable level of noise. It is noteworthy that the areas adjacent to the docks and port do not feature on any of the maps in Figure 7 as being quiet.

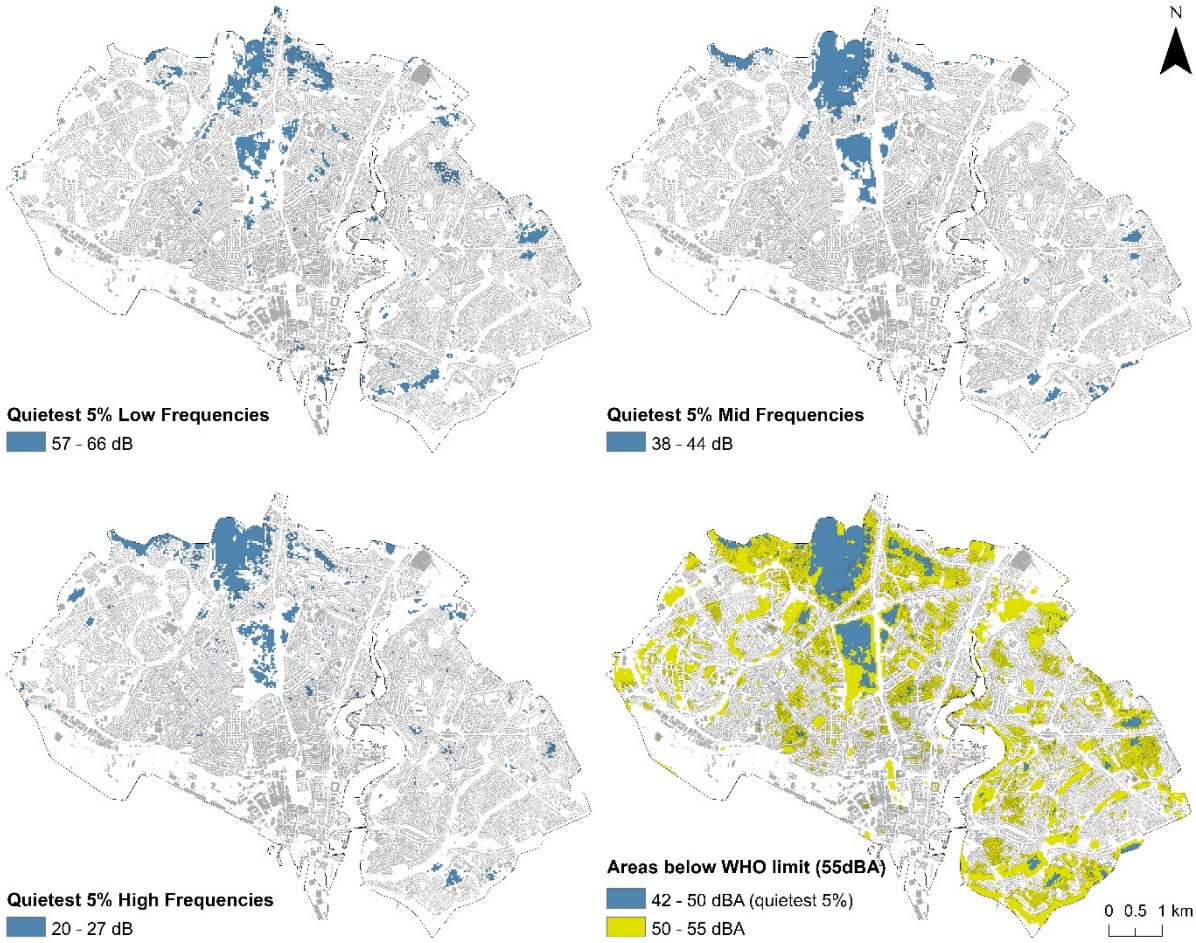

Figure 8. Quietest 5% of pixels in Southampton for low (top-left), mid (top-right), high (bottom-left) frequencies and dBA (bottom-right). The dBA map also shows areas meeting the 55 dBA daytime threshold specified in the END (in light green).

Looking at the opposite end of the noise scale, Figure 9 shows the loudest 5% of pixels for each frequency band and dBA. Here it is apparent that although the network of major roads marks the noisiest locations in the mid-frequencies and for dBA, it is the container port and its surroundings that dominate in the low frequency bands (Figure 9, top left). Probable sources of noise include ships manoeuvring into port, operations using cranes, and the mechanical sounds of shipping containers being loaded and unloaded (metal against metal or metal against tarmac). Such noises may also contain high frequencies (as Figure 9, bottom left, suggests), along with other sources such as the city centre and road traffic.

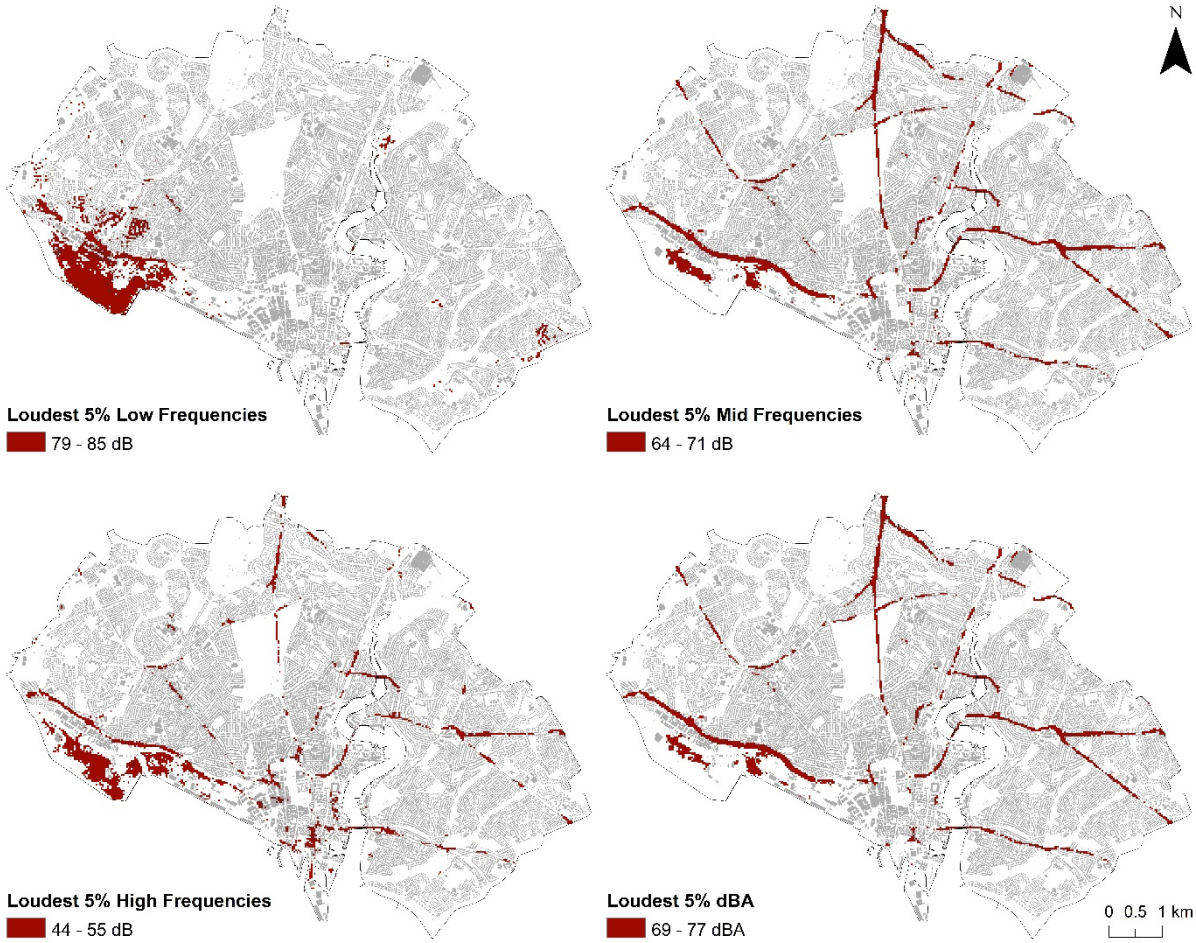

366

367 Figure 9. Loudest 5% of pixels in Southampton for the low (top-left), mid (top-right), high (bottom-
368 left) frequency bands and dBA (bottom-right).

369

370

371

Discussion and conclusions

Noise maps can be a powerful tool in the management and reduction of noise pollution in urban environments because they unveil spatial patterns in noise, identify who might be affected and can usefully inform citizens about their possible exposure. Yet conventional noise mapping, based on propagation models or interpolation of fixed-point measurements, has limitations that the survey and modelling approaches presented here overcome or provide a complementary methodology.

We used mobile surveys to gather more than 52,000 georeferenced audio recordings of ten seconds duration each and processed them to extract sound pressure levels (SPLs) in three frequency groupings and dBA. We then modelled the mean SPLs in 13,554 pixels as a function of urban form and traffic data, using a modern machine learning approach. By projecting these models to the entire study city at 30m resolution, we were able to create detailed noise maps for each frequency component. There are a number of benefits in this approach. First, by including all noise sources, our approach has advantages over noise maps created from simplified emission and propagation models, which are usually calculated from traffic flows on major roads, rail traffic and industrial sources, validated with a few noise measurements in the field (DEFRA 2015; McAlexander *et al.* 2015; Guillaume *et al.* 2019). Our coverage is more complete (e.g. not restricted to areas close to roads) and based on more empirical data than conventional noise mapping.

Second, our approach moves away from spatial interpolation techniques which, although widely used to determine noise levels, yield uncertainties. This is especially true if the resolution of the output is higher than that of the collected input data; if there are large areas without noise data, giving the interpolation nothing to work with (Asensio *et al.* 2011; Can *et al.* 2014); and where the urban environment between sampled points is variable. Methods that neglect features of urban form are missing major factors in the understanding of noise exposure at the street level (McAlexander *et al.* 2015) because urban noise is intrinsically spatial, varying depending on the locations of sources, receivers and the configuration of urban environment (e.g. building footprints and heights, vegetation, terrain geometry and other urban features that act as barriers). The use of machine learning approaches such as BRT to capture the relationships between noise data and the urban environment is key, not only because of strong predictive performance, but also because predictor variables of any type can be handled while dealing with complex, non-linear relationships and interactions. Torija and Ruiz (2015) have previously demonstrated that machine learning approaches achieve better predictive results for noise modelling than conventional statistical methods such as multiple linear regression.

To achieve the coverage needed to build these machine learning models, we needed measurements from many more locations than have often been used in past surveys, which typically rely on static recording stations (Murphy & King 2014a; McAlexander *et al.* 2015; Khan *et al.* 2018). Using static recording stations limits both the number and variety of locations sampled, making it impossible to capture real exposure experienced by individuals moving freely about a city. Indeed, as Tonne *et al.* (2018) note, there are very few studies that focus directly on personal exposure to noise, and this is one reason. Calculations used to create strategic noise maps for the purposes of the END, are generally based on data collected from static receivers located at 1.5 to 4 m height and at least 3 m away from hard surfaces, to reduce the effect of noise reflections (Murphy & King 2014). This approach may fail to capture real exposure experienced by pedestrians because they generally hear noise at somewhere between 1.5 m and 1.8 m height. Road traffic, one of the main sources of urban noise (King & Murphy 2016; Science for Environment Policy 2016; European Commission 2017; Khan *et al.* 2018), is also much closer to the ground than 4 m height. Furthermore, it is unrealistic to place microphones away from hard surfaces on the basis of reducing reflections because, in reality, noise experienced by individuals at the street level will always contain some noise that is reflected from a variety of hard surfaces. It has been suggested that strategic noise maps are beneficial because they enable EU state members to identify both the percentage of population being exposed to high levels of noise, and the areas of the urban agglomerations that need to be prioritised for environmental noise management (King & Murphy 2016). Yet these maps may be underestimating the levels of noise and the actual percentage of people being exposed.

Comparison of the official strategic noise map for the city of Southampton (DEFRA 2020a, b) (Figure 6, bottom row) and our outputs (Figures 6-9) exemplify the problems. While overall noise levels for the major roads are comparable, the strategic noise map does not calculate noise levels away from the road network, leaving much of the city where people live with no estimates. Furthermore, as their name suggests, strategic noise maps focus on noise (measured in dBA) and do not allow frequency components to be separated. As Figures 6-8 show, different frequency components may have different spatial patterns and the loud, low frequencies of the port are missing from the official mapping. Our maps for mid-frequencies and dBA are similar because this is where the A-weighting curve has least effect on the SPLs. At lower frequencies especially, A-weighting seriously down-weights the SPLs (e.g. by ~40 dB in the 22 to 44 Hz band). It must be questioned whether use of A-weighting for noise mapping makes sense if impacts on health are the main consideration. Persinger (2014) and Alves et al. (2018) note how A-weighting "disguises" and leads to "remarkable underestimation" of impacts at low frequencies. In the field, the underestimation of both low and high frequency noise may also be compounded by the relaxed tolerances permitted under international

standard IEC 61672-1:2013 on Class 1 measuring instruments used for environmental monitoring. For example, while at 1 kHz a tolerance of ± 1.1 dB is required, this is relaxed to -4.5 to + 2.5 dB at 16 Hz and to -17.0 to +3.5 dB at 16 kHz, raising the possibility of marked under or over-estimation outside the mid-frequency range.

It is also not possible to use strategic noise maps to identify the quietest urban areas with any accuracy, simply because they are away from major roads. This is despite the requirement for EU Member States to identify and preserve areas that are quiet and considered to be of good acoustic environmental quality, to protect the European Soundscape (European Environment Agency 2019). Using the models developed here, however, shows that the quietest areas in Southampton are mainly located in green areas or on natural land with a relative dense canopy of trees. The northern part of the city contains relatively large areas where the levels of noise are within the acceptable threshold as defined by the END (Figure 8). However, the south and south-western parts of the city provide few quiet areas, meaning that a significant number of residents are living with high levels of noise and with limited access to quieter areas near their homes. They are also exposed to significant noise from the port which continues day and night, yet shipping is excluded from much noise mapping.

An important issue with any environmental model is accuracy, but comparisons are difficult because strategic noise maps do not report predicted versus measured noise levels. Our models achieved r^2 values of 41% to 61% with mean absolute errors of 4.1 to 4.8 dB or dBA, depending on frequencies. While these values could probably be improved (e.g. by inclusion of additional predictor variables such as vehicle composition and road speed), they may be typical of noise models based on mobile surveys which achieve widespread coverage at the expense of long recording durations at single points. In other words, a mobile survey is less likely to capture temporal variations at a single point because the observer quickly moves on. Equally, adjacent short duration recordings from locations spaced only metres apart (and hence in essentially the same environment) may have quite different noise levels if sound sources are intermittent (such as passing traffic). The intermittency of sound sources in regression-type models of urban noise (including machine-learning approaches) leads to large residual error and therefore relatively low explained variance (r^2) and high mean absolute errors.

If mobile surveys have limitations yet wide coverage is needed, an alternative is to implement an integrated network of static sensors across a city, and this may be the future. The demands of real time data recording have pushed the boundaries of sensors and electronics making possible the development of smaller, cheaper and more energy efficient devices with embedded processing systems and wire/wireless communication systems. Environmental monitoring based on the Internet of Things (IoT) is now becoming common in areas such as transportation, temperature sensing,

atmospheric pollution monitoring and smart cities, among others (Marsal-Llacuna *et al.* 2014; Singleton *et al.* 2017; Hill *et al.* 2019). However, Picaut et al. (2020) note that although there is a great potential in the application of IoT to monitor urban noise, the implementation of an integrated system of sound sensors can be complex due to the requirement of a high density of sensors to capture spatial and temporal variability, and the need for advanced processing capabilities. Until such time, mobile surveys offer a way forward and methods developed to handle the big data that mobile sensors yield, such as those here, can equally be applied to data from future fixed sensor networks.

Acknowledgements

The authors should like to thank Jerome Kreule, Dominika Murienova and Rodrigo Batistela for help with the field surveys, funded by the Excel and University of Southampton Placement Schemes. Two reviewers provided useful comments on the manuscript.

Funding

This research formed part of Tatiana Alvares-Sanches's PhD project funded by the Engineering and Physical Sciences Research Council [EP/J017698/1, Transforming the Engineering of Cities to Deliver Societal and Planetary Wellbeing]

Author contributions

Tatiana Alvares-Sanches: Conceived and designed the study; organised, led and conducted fieldwork; cleaned and processed audio files; undertook the spatial and statistical data analysis and data visualisation outputs; wrote the original draft and incorporated revisions. **Patrick E. Osborne:** Contributed to the design of the fieldwork and participated in the data collection campaign; edited and contributed to the writing of the article. **Paul R. White:** Contributed to the design of the fieldwork; wrote the original MATLAB® routine to process the audio files; reviewed the article.

References

Abramic, A., Kotsev, A., Cetl, V., Kephalopoulos, S. & Paviotti, M. 2017. A spatial data infrastructure for environmental noise data in Europe. *International Journal of Environmental Research and Public Health*, **14**, https://doi.org/10.3390/ijerph14070726.

Alvares-Sanches, T., Osborne, P.E., White, P. & Bahaj, A. 2019. Spatial Variation in Sound Frequency Components Across an Urban Area Derived from Mobile Surveys. *Future Cities and Environment*, **5**, 1–17, https://doi.org/https://doi.org/10.5334/fce.54 TECHNICAL.

Alves, J.A., Silva, L.T. & Remoaldo, P.C. 2018. Impacts of Low Frequency Noise Exposure on Well-Being: A Case-Study From Portugal. *Noise and Health*, **20**, 131–145.

Andersson, E.M., Ögren, M., Molnár, P., Segersson, D., Rosengren, A. & Stockfelt, L. 2020. Road traffic noise, air pollution and cardiovascular events in a Swedish cohort. *Environmental Research*, **185**, 109446, https://doi.org/10.1016/j.envres.2020.109446.

Asensio, C., Ruiz, M., Pavón, I., Ausejo, M. & Recuero, M. 2011. Uncertainty in noise maps isolines: The effect of the sampling grid. *Acta Acustica united with Acustica*, **97**, 237–242, https://doi.org/10.3813/AAA.918403.

Badino, A., Borelli, D., Gaggero, T., Rizzuto, E. & Schenone, C. 2016. Airborne noise emissions from ships: Experimental characterization of the source and propagation over land. *Applied Acoustics*, **104**, 158–171, https://doi.org/10.1016/j.apacoust.2015.11.005.

Beutel, M.E., Jünger, C., et al. 2016. Noise annoyance is associated with depression and anxiety in the general population - the contribution of aircraft noise. *PLoS ONE*, **11**, 1–10, https://doi.org/10.1371/journal.pone.0155357.

Bouzir, T.A.K. & Zemmouri, N. 2017. Effect of urban morphology on road noise distribution. *Energy Procedia*, **119**, 376–385, https://doi.org/10.1016/j.egypro.2017.07.121.

Brown, A.L. 2015. Effects of Road Traffic Noise on Health: From Burden of Disease to Effectiveness of Interventions. *Procedia Environmental Sciences*, **30**, 3–9, https://doi.org/10.1016/j.proenv.2015.10.001.

Cai, M., Zou, J., Xie, J. & Ma, X. 2015. Road traffic noise mapping in Guangzhou using GIS and GPS. *Applied Acoustics*, **87**, 94–102, https://doi.org/10.1016/j.apacoust.2014.06.005.

Can, A., Dekoninck, L. & Botteldooren, D. 2014. Measurement network for urban noise assessment: Comparison of mobile measurements and spatial interpolation approaches. *Applied Acoustics*, **83**, 32–39, https://doi.org/10.1016/j.apacoust.2014.03.012.

Castelo Branco, N.A.A. 2001. Low frequency noise A major risk factor in military operations. *In*: *The RTO AVT Symposium on "Ageing Mechanisms and Control:Part A – Developments in Computational Aero- and Hydro-Acoustics", and Published in RTO-MP-079(I)*. Manchester, UK, 12.

Chetoni, M., Ascari, E., Bianco, F., Fredianelli, L., Licitra, G. & Cori, L. 2016. Global noise score indicator for classroom evaluation of acoustic performances in LIFE GIOCONDA project. *Noise Mapping*, **3**, 157–171, https://doi.org/10.1515/noise-2016-0012.

DEFRA. 2015. *Strategic Noise Mapping: Explaining Which Noise Sources Were Included in 2012 Noise Maps*.

DEFRA. 2016. Noise mapping Englandhttp://services.defra.gov.uk/wps/portal/noise/about.

DEFRA. 2020a. Road Noise - Lden - England Round 3. *Department for Environment, Food and Rural Affairs*https://data.gov.uk/dataset/d53bd2bb-2fe8-450f-b435-851e46ec7e92/road-noise-lden-england-round-3.

DEFRA. 2020b. Road Noise - Lnight - England Round 3. *Department for Environment, Food and Rural Affairs*https://data.gov.uk/dataset/4ab55650-a3e7-4132-a968-4cd67fe79135/road-noise-lnight-england-round-3.

Díaz, J., López-Bueno, J.A., López-Ossorio, J.J., Gónzález, J.L., Sánchez, F. & Linares, C. 2020. Short-term effects of traffic noise on suicides and emergency hospital admissions due to anxiety and depression in Madrid (Spain). *Science of the Total Environment*, **710**, 136315, https://doi.org/10.1016/j.scitotenv.2019.136315.

Dons, E., Van Poppel, M., Kochan, B., Wets, G. & Int Panis, L. 2013. Modeling temporal and spatial variability of traffic-related air pollution: Hourly land use regression models for black carbon. *Atmospheric Environment*, **74**, 237–246, https://doi.org/10.1016/j.atmosenv.2013.03.050.

Dons, E., Van Poppel, M., Int Panis, L., De Prins, S., Berghmans, P., Koppen, G. & Matheeussen, C. 2014. Land use regression models as a tool for short, medium and long term exposure to traffic related air pollution. *Science of The Total Environment*, **476–477**, 378–386, https://doi.org/10.1016/j.scitotenv.2014.01.025.

Douglas, O. & Murphy, E. 2016. Source-based subjective responses to sleep disturbance from transportation noise. *Environment International*, **92–93**, 450–456, https://doi.org/10.1016/j.envint.2016.04.030.

EC. 2015. *Commission Directive (EU) 2015/ 996 of 19 May 2015 Establishing Common Noise Assessment Methods According to Directive 2002/49/EC of the European Parliament and of the Council*.

EEA. 2014. *Noise in Europe 2014*. Copenhagen, https://doi.org/10.2800/763331.

EEA. 2019. *Road Traffic Remains Biggest Source of Noise Pollution in Europe*.

Elith, J. & Leathwick, J.R. 2017. Boosted Regression Trees for ecological modeling. *Vignette BRT package*, 1–22.

Elith, J., Leathwick, J.R. & Hastie, T. 2008a. A working guide to boosted regression trees. *Journal of Animal Ecology*, **77**, 802–813, https://doi.org/10.1111/j.1365-2656.2008.01390.x.

Elith, J., Leathwick, J.R. & Hastie, T. 2008b. Appendix S1: Explanation of the effect of learning rate on predictive stability in boosted regression trees. *Journal of Animal Ecology*, **77**, 802–813, https://doi.org/10.1111/j.1365-2656.2008.01390.x.

European Commission. 2017. *Science for Environment Policy FUTURE BRIEF: Noise Abatement Approaches*, https://doi.org/10.2779/016648.

European Environment Agency. 2019. *Environmental Noise in Europe - 2020*, https://doi.org/10.2800/686249.

Fletcher, M.D., Lloyd Jones, S., White, P.R., Dolder, C.N., Leighton, T.G. & Lineton, B. 2018. Effects of very high-frequency sound and ultrasound on humans. Part II: A double-blind randomized provocation study of inaudible 20-kHz ultrasound. *The Journal of the Acoustical Society of America*, **144**, 2521–2531, https://doi.org/10.1121/1.5063818.

Fredianelli, L., Del Pizzo, A. & Licitra, G. 2019. Recent developments in sonic crystals as barriers for road traffic noise mitigation. *Environments - MDPI*, **6**, 1–19, https://doi.org/10.3390/environments6020014.

583 Friedman, J.H. 2001. Greedy Function Approximation: A Gradient Boosting Machine. *Annals of*
584 *Statistics*, **29**, 1189–1232, https://doi.org/10.1214/009053606000000795.

585 Goldsmith, M. 2012. *Discord: The Story of Noise*. Oxford, Oxford University Press.

586 Greenwell, B., Boehmke, B. & Cunningham, J. 2018. *Package 'Gbm' - Generalized Boosted Regression*
587 *Models*. **2.1.4**.

588 Grus, J. 2015. *Data Science from Scratch: First Principles with Python*, 1st ed. Beaugureau, M. (ed.).
589 Sebastopol, O'Reilly Media.

590 Guillaume, G., Aumond, P., Chobeau, P. & Can, A. 2019. Statistical study of the relationships between
591 mobile and fixed stations measurements in urban environment. *Building and Environment*, **149**,
592 404–414, https://doi.org/10.1016/j.buildenv.2018.12.014.

593 Gulliver, J., Morley, D., et al. 2015. Development of an open-source road traffic noise model for
594 exposure assessment. *Environmental Modelling & Software*, **74**, 183–193,
595 https://doi.org/10.1016/j.envsoft.2014.12.022.

596 Guski, R., Klatte, M., Moehler, U., Müller, U., Nieden, A. Zur & Schreckenberg, D. 2016. NORAH (Noise
597 Related Annoyance, Cognition, and Health): Questions, designs, and main results. *In*: *Procedings*
598 *of the 22nd International Congress on Acoustics*. Buenos Aires, 0–6.

599 Han, X., Huang, X., Liang, H., Ma, S. & Gong, J. 2018. Analysis of the relationships between
600 environmental noise and urban morphology. *Environmental Pollution*, **233**, 755–763,
601 https://doi.org/10.1016/j.envpol.2017.10.126.

602 Hastie, T., Tibsharani, R. & Friedman, J. 2009. *The Elements of Statistical Learning. Data Mining,*
603 *Inference, and Prediction*, 2nd ed. New York, Springer-Verlag New York,
604 https://doi.org/10.1007/978-0-387-84858-7.

605 Hill, A.P., Prince, P., Snaddon, J.L., Doncaster, C.P. & Rogers, A. 2019. AudioMoth: A low-cost acoustic
606 device for monitoring biodiversity and the environment. *HardwareX*, **6**, 1–19,
607 https://doi.org/10.1016/j.ohx.2019.e00073.

608 Hong, J.Y. & Jeon, J.Y. 2017. Exploring spatial relationships among soundscape variables in urban areas:
609 A spatial statistical modelling approach. *Landscape and Urban Planning*, **157**, 352–364,
610 https://doi.org/10.1016/j.landurbplan.2016.08.006.

611 James, G., Witten, D., Hastie, T. & Tibshirani, R. 2017. *An Introduction to Statistical Learning with*
612 *Applications in R*, 8th ed. New York, Springer, https://doi.org/10.1016/j.peva.2007.06.006.

613 Kardous, C.A. & Shaw, P.B. 2016. Evaluation of smartphone sound measurement applications (apps)
614 using external microphones—A follow-up study . *The Journal of the Acoustical Society of*
615 *America*, **140**, EL327–EL333, https://doi.org/10.1121/1.4964639.

616 Kephalopoulos, S., Paviotti, M., Anfosso-Lédée, F., Van Maercke, D., Shilton, S. & Jones, N. 2014.
617 Advances in the development of common noise assessment methods in Europe: The CNOSSOS-
618 EU framework for strategic environmental noise mapping. *Science of the Total Environment*,
619 **482**–**483**, 400–410, https://doi.org/10.1016/j.scitotenv.2014.02.031.

620 Khan, J., Ketzel, M., Kakosimos, K., Sørensen, M. & Jensen, S.S. 2018. Road traffic air and noise
621 pollution exposure assessment – A review of tools and techniques. *Science of the Total*
622 *Environment*, **634**, 661–676, https://doi.org/10.1016/j.scitotenv.2018.03.374.

623 King, E.A. & Murphy, E. 2016. Environmental noise - 'Forgotten' or 'Ignored' pollutant? *Applied*
624 *Acoustics*, **112**, 211–215, https://doi.org/10.1016/j.apacoust.2016.05.023.

Kumar, K., Ledoux, H., Schmidt, R., Verheij, T. & Stoter, J. 2020. A harmonized data model for noise simulation in the EU. *ISPRS International Journal of Geo-Information*, **9**, https://doi.org/10.3390/ijgi9020121.

Laszlo, H.E., McRobie, E.S., Stansfeld, S.A. & Hansell, A.L. 2012. Annoyance and other reaction measures to changes in noise exposure - A review. *Science of the Total Environment*, **435**–**436**, 551–562, https://doi.org/10.1016/j.scitotenv.2012.06.112.

Leighton, T.G. 2016. Are some people suffering as a result of increasing mass exposure of the public to ultrasound in air? *Proceedings of the Royal Society A*, **472**, https://doi.org/dx.doi.org/10.1098/rspa.2015.0624.

Lercher, P., Evans, G.W. & Meis, M. 2003. Ambient noise and cognitive processes among primary schoolchildren. *Environment and Behavior*, **35**, 725–735, https://doi.org/10.1177/0013916503256260.

Licitra, G., Bolognese, M., Palazzuoli, D., Fredianelli, L. & Fidecaro, F. 2019. Port noise impact and citizens' complaints evaluation in rumble and mon acumen interreg projects. *Proceedings of the 26th International Congress on Sound and Vibration, ICSV 2019*.

Marsal-Llacuna, M.L., Colomer-Llinàs, J. & Meléndez-Frigola, J. 2014. Lessons in urban monitoring taken from sustainable and livable cities to better address the Smart Cities initiative. *Technological Forecasting and Social Change*, **90**, 611–622, https://doi.org/10.1016/j.techfore.2014.01.012.

McAlexander, T.P., Gershon, R.R.M. & Neitzel, R.L. 2015. Street-level noise in an urban setting: assessment and contribution to personal exposure. *Environmental Health*, **14**, 18, https://doi.org/10.1186/s12940-015-0006-y.

Merchant, N.D., Fristrup, K.M., Johnson, M.P., Tyack, P.L., Witt, M.J., Blondel, P. & Parks, S.E. 2015. Measuring acoustic habitats. *Methods in Ecology and Evolution*, **6**, 257–265, https://doi.org/10.1111/2041-210X.12330.

Monrad, M., Sajadieh, A., et al. 2016. Residential exposure to traffic noise and risk of incident atrial fibrillation: A cohort study. *Environment International*, **92**–**93**, 457–463, https://doi.org/10.1016/j.envint.2016.04.039.

Morel, J., Marquis-Favre, C. & Gille, L.A. 2016. Noise annoyance assessment of various urban road vehicle pass-by noises in isolation and combined with industrial noise: A laboratory study. *Applied Acoustics*, **101**, 47–57, https://doi.org/10.1016/j.apacoust.2015.07.017.

Murphy, E. & King, E. 2014a. *Environmental Noise Pollution Noise Mapping, Public Health, and Policy*, 1st ed. Amsterdam, Elsevier.

Murphy, E. & King, E.A. 2014b. An assessment of residential exposure to environmental noise at a shipping port. *Environment International*, **63**, 207–215, https://doi.org/10.1016/j.envint.2013.11.001.

Murphy, E. & King, E.A. 2016. Smartphone-based noise mapping: Integrating sound level meter app data into the strategic noise mapping process. *Science of the Total Environment*, **562**, 852–859, https://doi.org/10.1016/j.scitotenv.2016.04.076.

Murphy, E., Faulkner, J.P. & Douglas, O. 2020. Current State-of-the-Art and New Directions in Strategic Environmental Noise Mapping. *Current Pollution Reports*, **6**, 54–64, https://doi.org/10.1007/s40726-020-00141-9.

Persinger, M.A. 2014. Infrasound, human health, and adaptation: An integrative overview of recondite

668 hazards in a complex environment. *Natural Hazards*, **70**, 501–525,
669 https://doi.org/10.1007/s11069-013-0827-3.

670 Picaut, J., Can, A., Fortin, N., Ardouin, J. & Lagrange, M. 2020. Low-cost sensors for urban noise
671 monitoring networks—A literature review. *Sensors (Switzerland)*, **20**,
672 https://doi.org/10.3390/s20082256.

673 Ricciardi, P., Delaitre, P., Lavandier, C., Torchia, F. & Aumond, P. 2015. Sound quality indicators for
674 urban places in Paris cross-validated by Milan data. *The Journal of the Acoustical Society of*
675 *America*, **138**, 2337–2348, https://doi.org/10.1121/1.4929747.

676 Sakieh, Y., Jaafari, S., Ahmadi, M. & Danekar, A. 2017. Green and calm: Modeling the relationships
677 between noise pollution propagation and spatial patterns of urban structures and green covers.
678 *Urban Forestry and Urban Greening*, **24**, 195–211, https://doi.org/10.1016/j.ufug.2017.04.008.

679 Schenone, C., Pittaluga, I., Borelli, D., Kamali, W. & El Moghrabi, Y. 2016. The impact of environmental
680 noise generated from ports: Outcome of MESP project. *Noise Mapping*, **3**, 26–36,
681 https://doi.org/10.1515/noise-2016-0002.

682 Scholkmann, F. 2019. Exposure to High-Frequency Sound and Ultrasound in Public Places: Examples
683 from Zurich, Switzerland. *Acoustics*, **1**, 816–824, https://doi.org/10.3390/acoustics1040048.

684 Science for Environment Policy. 2016. *Links between Noise and Air Pollution and Socioeconomic Status*.
685 Bristol, https://doi.org/ISBN 978-92-79-45734-0\rISSN 2363-2798\rDOI 10.2779/200217.

686 Singleton, A.D., Spielman, S.E. & Folch, D.C. 2017. *Urban Analytics*, 1st ed. London, SAGE Publications
687 Ltd.

688 Smith, R.B., Beevers, S.D., et al. 2020. Impacts of air pollution and noise on risk of preterm birth and
689 stillbirth in London. *Environment International*, **134**, 105290,
690 https://doi.org/10.1016/j.envint.2019.105290.

691 Sørensen, M., Andersen, Z.J., et al. 2012. Road traffic noise and incident myocardial infarction: A
692 prospective cohort study. *PLoS ONE*, **7**, 1–7, https://doi.org/10.1371/journal.pone.0039283.

693 Tonne, C., Milà, C., et al. 2018. Socioeconomic and ethnic inequalities in exposure to air and noise
694 pollution in London. *Environment International*, **115**, 170–179,
695 https://doi.org/10.1016/j.envint.2018.03.023.

696 Torija, A.J. & Ruiz, D.P. 2015. A general procedure to generate models for urban environmental-noise
697 pollution using feature selection and machine learning methods. *Science of the Total*
698 *Environment*, **505**, 680–693, https://doi.org/10.1016/j.scitotenv.2014.08.060.

699 van Kempen, E. & Babisch, W. 2012. The quantitative relationship between road traffic noise and
700 hypertension: a meta-analysis. *Journal of Hypertension*, **30**, 1075–1086.

701 van Kempen, E., Casas, M., Pershagen, G. & Foraster, M. 2018. WHO environmental noise guidelines
702 for the European region: A systematic review on environmental noise and cardiovascular and
703 metabolic effects: A summary. *International Journal of Environmental Research and Public*
704 *Health*, **15**, 1–59, https://doi.org/10.3390/ijerph15020379.

705 Wang, V.S., Lo, E.W., Liang, C.H., Chao, K.P., Bao, B.Y. & Chang, T.Y. 2016. Temporal and spatial
706 variations in road traffic noise for different frequency components in metropolitan Taichung,
707 Taiwan. *Environmental Pollution*, **219**, 174–181, https://doi.org/10.1016/j.envpol.2016.10.055.

708 Weber, N., Haase, D. & Franck, U. 2014. Assessing modelled outdoor traffic-induced noise and air
709 pollution around urban structures using the concept of landscape metrics. *Landscape and Urban*
710 *Planning*, **125**, 105–116, https://doi.org/10.1016/j.landurbplan.2014.02.018.

WHO. 2018. *Environmental Noise Guidelines for the European Region*. Copenhagen, Denmark, WHO Regional Office for Europe.

Zhang, M.Y., Chen, C., Xie, X.J., Xu, S.L., Guo, G.Z. & Wang, J. 2016. Damage to Hippocampus of Rats after Being Exposed to Infrasound. *Biomedical and Environmental Sciences*, **29**, 435–442, https://doi.org/10.3967/bes2016.056.